

# Time dependence of laser cooling in optical lattices

Claude M. Dion,\* Peder Sjölund, Stefan J. H. Petra, Svante Jonsell, and Anders Kastberg  
*Department of Physics, Umeå University, SE-901 87 Umeå, Sweden*

We study the dynamics of the cooling of a gas of caesium atoms in an optical lattice, both experimentally and with 1D full-quantum Monte Carlo simulations. We find that, contrary to the standard interpretation of the Sisyphus model, the cooling process does not work by a continuous decrease of the average kinetic energy of the atoms in the lattice. Instead, we show that the momentum of the atoms follows a bimodal distribution, the atoms being gradually transferred from a hot to a cold mode. We suggest that the cooling mechanism should be depicted in terms of a rate model, describing the transfer between the two modes along with the processes occurring within each mode.

PACS numbers: 32.80.Pj, 05.10.Ln

## I. INTRODUCTION

Laser cooling is now a well-established technique enabling to reach temperatures of the order of the microkelvin in a gas of atoms [1]. It has made possible Bose-Einstein condensation [2], while laser-cooled atoms are used, for instance, in atomic clocks [3] and as frequency standards [4], and have been proposed for parity violation measurements [5] and quantum information processing [6].

An appropriate superposition of laser beams can result in a spatially-periodic modulation of the polarisation of the light, creating an optical lattice [7, 8, 9]. A multilevel atom with a degenerate ground state moving through such a lattice will experience large non-adiabatic effects as the light shift of the different substates and the optical pumping rates then depend on the position of the atom. The standard model used to explain laser cooling in optical lattices is Sisyphus cooling [10, 11], where an atom will preferentially jump from the crest of a potential hill to the valley of an other potential, losing kinetic energy each time. Atom dynamics can be expressed in a semi-classical way by this model as the interplay between a velocity-dependent cooling force due to the Sisyphus effect and a diffusion term describing the recoil from photon absorption-emission cycles along with fluctuations in the gradient force when going from one potential curve to the other [10, 11].

Although it was predicted many years ago [10], it is only recently that experimental observations have shown non-Gaussian velocity distributions in optical lattices [12], as well as in atomic fountains [13]. While the standard Sisyphus model considers a cooling force linear in velocity [11], leading to a Gaussian momentum distribution, refinements using non-linear forces [10, 14] give non-Gaussian distributions, following for instance Tsallis or Lévy statistics [15, 16]. Results obtained by taking into account the localisation of the atoms around the potential minima also show deviations from a Gaussian [17, 18]. Moreover, arguments based on a “band” picture of optical lattices [19], where some atoms are trapped in the potential wells of the lattice while others move around in the “conduction band”, call for a bimodal distribution [12, 20]. Indeed, it was found that a double Gaussian function provides the best fit to both experimental and simulated data for the steady state momentum distribution of atoms [12].

We report in this letter a study of the time evolution of the cooling of a gas of caesium atoms inside an optical lattice. It provides new elements to understand the origin of the non-Gaussian momentum distributions. Apart from a few studies concerning localisation [21, 22], diffusion [23], and damping rates [24, 25] of atoms in optical lattices, this is one of the first observation of the dynamics of the cooling process.

## II. METHODOLOGY

Details of the experimental setup can be found in refs. [26, 27]. Briefly, we first accumulate  $^{133}\text{Cs}$  atoms in a magneto-optical trap. We adjust the irradiance and the detuning, then we turn off the magnetic field and leave the atoms in an optical molasses with even further reduced irradiance and increased detuning. The atoms are thus cooled to about  $40\ \mu\text{K}$  before being transferred to the optical lattice; such a “hot” initial cloud of atoms is used to reduce the effects from the initial kick given to the atoms when the lattice is turned on. The lattice itself has a 3D structure

---

\*Electronic address: claudedion@tp.umu.se

made up from a four-beam configuration [7, 9]: two laser beams are linearly polarised along the  $x$  axis and propagate in the  $yz$  plane symmetrically with respect to the  $z$  axis, whereas the other two beams are polarised along the  $y$  axis and propagate in the  $xz$  plane symmetrically with respect to  $z$ . This yields a tetragonal pattern of points with pure circular polarisation, alternately  $\sigma^+$  and  $\sigma^-$ . The lasers are slightly detuned below the resonance of the  $F_g = 4 \rightarrow F_e = 5$  transition of the D2 line ( $6s^2S_{1/2} \rightarrow 6p^2P_{3/2}$ ) at  $\lambda = 852$  nm. After a given time the optical lattice is turned off (in  $4.2 \mu\text{s}$ ) and the atoms are left to fall and then detected by a probe beam located  $\sim 5$  cm below the trapping region. This turn-off time is fast enough so that no adiabatic cooling of the atomic cloud can occur. The momentum distribution of the atoms is recovered from the time-of-flight signal.

The simulation of the dynamics of the atoms in the optical lattice is carried out using a full-quantum Monte Carlo wave-function method [28] for the  $F_g = 4 \rightarrow F_e = 5$  transition of caesium [12]. Due to the numerical complexity of the 3D case, we restrict ourselves to a 1D lin  $\perp$  lin configuration, reproducing the same alternation of  $\sigma^+$  and  $\sigma^-$  potential wells (see, *e.g.*, ref. [8]). The time dependence of the cooling process is obtained by considering a series of different histories where the initial momentum of the atom is chosen randomly from a normal distribution corresponding to a temperature of  $50 \mu\text{K}$ . Observables are recovered by averaging over these histories, *e.g.*, the momentum distribution is obtained from the time-dependent wave functions  $\psi_h$  by

$$D(p; t) = \frac{1}{N} \sum_{h=1}^N |\psi_h(p; t)|^2, \quad (1)$$

where the index  $h$  labels the different histories.

### III. RESULTS

Sample momentum distributions obtained by the numerical simulation are given in fig. 1, for a detuning of  $\Delta = -10\Gamma$  and a potential well depth of  $U_0 = 127E_r$ , with  $\Gamma/2\pi = 5.2227$  MHz the natural linewidth of the  $6p^2P_{3/2}$  level of caesium and  $E_r = \hbar\omega_r$  the recoil energy, where  $\omega_r/2\pi = 2.0663$  kHz is the atomic recoil frequency [29]. The momentum is expressed in units of the recoil momentum  $p_r = \hbar/\lambda$ . Starting from the initial distribution at  $50 \mu\text{K}$ , we clearly see that a narrow peak gradually grows in the centre of the momentum distribution. At the same time, the population of the wings from the initial distribution decreases and spreads out to higher momentum. It appears that the atoms are not gradually cooled but populate progressively the central feature: they are transferred from a “hot” to a “cold” mode. To analyse these results, we have fitted the momentum distribution to a double Gaussian,

$$D(p) = A_{\text{cold}} \exp[-p^2 / (2\sigma_{\text{cold}}^2)] + A_{\text{hot}} \exp[-p^2 / (2\sigma_{\text{hot}}^2)], \quad (2)$$

by finding the parameters ( $A$  and  $\sigma$ ) that best reproduce the second,  $\langle p^2 \rangle$ , and fourth,  $\langle p^4 \rangle$ , moments of the distribution while conserving the norm, with the constraint  $\sigma_{\text{cold}} < \sigma_{\text{hot}}$ . This method appears better suited than the traditional  $\chi^2$  fitting procedure to reproduce the wings of the distribution when the cold mode dominates. We find, fig. 2(a), that there is no time evolution of the width  $\sigma_{\text{cold}}$ , hence we can assign a temperature  $T_{\text{cold}} = \sigma_{\text{cold}}^2 / (mk_B)$  to the cold mode, where  $m$  is the mass of the atom and  $k_B$  the Boltzmann constant. This is another striking feature of the cooling process, which works not only by transferring atoms between the two modes, but puts them in an *unchanging* cold mode. On the other hand, atoms in the hot mode are continuously heated. We have checked that no steady state is obtained in the hot mode for longer times. For as long as we can see, the momentum distribution in the hot mode shows a Gaussian profile in the region where it can clearly be distinguished from the cold mode. In contrast, as can be seen in fig. 2(b), the relative population of each mode (calculated as  $\sqrt{2\pi}A\sigma$  for a normalised distribution) reaches a steady state after some time. By fitting the population of the cold mode to an exponential function, we recover a transfer rate of  $\tau^{-1} \approx 7.9 \times 10^2 \text{ s}^{-1}$ . This rate is about 15 times slower than the localisation rate previously measured for caesium in a 1D lattice [21] and 2 orders of magnitude slower than the scattering rate. The persistence of hot atoms seems to be due to the fact that some higher momentum atoms are heated and never cooled. Indeed, starting from a lower temperature such as  $5 \mu\text{K}$  leads to a greater transfer from the hot to the cold mode, with less heating in the hot mode.

Turning now to the experimental results, we show in fig. 3 the momentum distribution obtained for a laser detuning of  $\Delta = -12.6\Gamma$  and an irradiance corresponding to a potential depth  $U_0 = 217E_r$ . (Since the simulation is for a 1D lattice, a quantitative comparison to the experiment is not meaningful, so no attempt is made to exactly match the parameters for both cases.) We see again the appearance of a central feature of almost constant width. The main difference with the simulation is that after a certain time the signal decreases, as seen in fig. 3(b). This is due to an overall loss of atoms due to their diffusion out of the lattice and collisions with background gas, while the numerical simulation considers an effectively infinite lattice. This phenomenon is probably also responsible for another difference

between the two results, namely the absence in the experimental signal of a significant heating of the hot mode, as the high momentum atoms seen in the simulation would quickly escape from the lattice region.

The result obtained by fitting the experimental data to a double Gaussian is given in fig. 4. Where have reverted here to a  $\chi^2$  method as a fit using the moments of the distribution gave aberrant results due to the bump present in the experimental data at negative momentum. It is clear from the time evolution of  $\sigma_{\text{hot}}$  (although it is noisy) that there is no heating observed in the hot mode. This is nevertheless not necessarily contradictory with the result of the simulation, as the decrease  $\sigma_{\text{hot}}$  could be explained by the preferential loss of the high momentum atoms. The temperature in the cold mode is almost constant, the slight decrease with time being within the experimental and fitting errors. The relative populations of the two modes shown in fig. 4(b) seem to indicate that a steady state is not reached, with the cold mode continuously gaining in population, which would indicate that the loss of atoms is through the hot mode. The rate of transfer to the cold mode is found to be of the same order as for the simulation, with  $\tau^{-1} \approx 5.8 \times 10^2 \text{ s}^{-1}$ , which is 6 times slower than the localisation rate in a 3D lattice [21] and  $\sim 400$  times slower than the scattering rate.

We ran simulations over a range of the parameters  $\Delta$  and  $U_0$  and the temperatures thus obtained for the cold mode are given in fig. 5. The variation of  $T_{\text{cold}}$  as a function of the well depth looks similar to that obtained in previous studies [12, 19, 23], although the temperature was then calculated from the root-mean-square momentum. It also appears that the temperature does not follow the linear dependence with potential depth predicted by an analytical model of Sisyphus cooling [30] for the entire range considered here. We also note that no *décrochage* is seen, *i.e.*, there is no threshold potential below which there would be a rapid increase of the temperature. The curve of fig. 5(a) is in fact similar to the results previously obtained by considering not the r.m.s. momentum, but the width of the distribution at  $1/\sqrt{e}$  [12, 19]. The dominance of the cold mode over the hot mode is such that the width at  $1/\sqrt{e}$  is essentially equal to  $\sigma_{\text{cold}}$ , except for very short times. It thus seems that the previously observed *décrochage* appears when the population of the hot mode is great enough to influence significantly the r.m.s. momentum. It is a feature of the relative population of the modes, not of the cooling temperature reached. Extrapolating to a vanishing potential depth results in a non-zero value of  $T_{\text{cold}}$ , but we expect the behaviour to become non linear as the number of bound states in the lattice goes to zero. The temperature of the cold mode also varies with the detuning, as shown in fig. 5(b). This is consistent with what has been observed for rubidium [23, 25], although it appears that  $T_{\text{cold}}$  decreases exponentially with  $|\Delta|$ , instead of following the functional form proposed in refs. [23, 25].

#### IV. DISCUSSION

Our results call for a discussion of the cooling of atoms in optical lattices in terms of rates for a bimodal distribution, based on the hypothesis that the cold and hot modes correspond to trapped and untrapped atoms, respectively. The dominant process during the initial cooling stage is the transfer from the hot to the cold mode. Within the hot mode, simulations show that there is an important heating effect, while for the cold mode basically no heating or cooling is seen, which means that there is a fast equilibrium reached inside the cold mode. This latter process depends on the detuning of the lasers, as seen by the dependence of  $T_{\text{cold}}$  not only on the potential depth but also on the detuning. There is also the transfer from the cold to the hot mode, which, according to simulations, is slow with respect to the transfer from hot to cold. Otherwise, there would be a gradual depletion of the cold mode as atoms in the hot mode are heated to the extent where they cannot go back to the cold mode. Nevertheless, under the hypothesis that cold atoms are trapped, the loss of atoms due to diffusion could only be explained by a coupling from cold to hot. We also note that associating the cold mode with trapped atoms is not incompatible with the observation that localisation is faster than cooling, as atoms can spend more time near the potential minima (*i.e.*, localise) while still being untrapped. In addition, the rate actually measured in ref. [21] may also reflect the progressive filling of lattice sites.

#### V. CONCLUSION

To summarise, we have shown that atoms in an optical lattice follow a bimodal distribution of hot and cold atoms. The cooling inside the lattice takes place via a transfer of the atoms from the hot to the cold mode. We suggest that the cooling of atoms in an optical lattice be depicted in terms of a rate model, describing the transfer between the two modes along with the processes occurring within each mode. This calls for further investigations in order to understand by exactly which mechanism this is taking place.

## Acknowledgments

We thank R. Kaiser, E. Lutz, K. Mølmer, and L. Sanchez-Palencia for stimulating discussions. This work was supported by Carl Tryggers stiftelse, Magnus Bergvalls stiftelse, Kempestiftelserna, K & A Wallenbergs stiftelse, and the Swedish Research Council. S.J.H.P. thanks Carl Tryggers stiftelse for financial support. This research was conducted using the resources of the High Performance Computing Center North (HPC2N).

- 
- [1] S. Chu, *Rev. Mod. Phys.* **70**, 685 (1998); W. D. Phillips, *ibid.* **70**, 707 (1998); C. Cohen-Tannoudji, *ibid.* **70**, 721 (1998).
  - [2] E. A. Cornell and C. E. Wieman, *Rev. Mod. Phys.* **74**, 875 (2002); W. Ketterle, *ibid.* **74**, 875 (2002).
  - [3] S. Bize, P. Laurent, M. Abgrall, H. Marion, I. Maksimovic, L. Cacciapuoti, J. Grünert, C. Vian, F. Pereira dos Santos, P. Rosenbusch, P. Lemonde, G. Santarelli, P. Wolf, A. Clairon, A. Luiten, M. Tobar, and C. Salomon, *J. Phys. B: At., Mol. Opt. Phys.* **38**, S449 (2005).
  - [4] L. Hollberg, C. W. Oates, G. Wilpers, C. W. Hoyt, Z. W. Barber, S. A. Diddams, W. H. Oskay, and J. C. Bergquist, *J. Phys. B: At., Mol. Opt. Phys.* **38**, S649 (2005).
  - [5] S. Sanguinetti, J. Guéna, M. Lintz, P. Jacquier, A. Wasan, and M.-A. Bouchiat, *Eur. Phys. J. D* **25**, 3 (2003).
  - [6] C. Monroe, *Nature* **416**, 238 (2002).
  - [7] P. Jessen and I. Deutsch, *Adv. At. Mol. Opt. Phys.* **37**, 95 (1996).
  - [8] L. Guidoni and P. Verkerk, *J. Opt. B.: Quantum Semiclass. Opt.* **1**, R23 (1999).
  - [9] G. Grynberg and C. Robilliard, *Phys. Rep.* **355**, 335 (2001).
  - [10] Y. Castin, J. Dalibard, and C. Cohen-Tannoudji, in *Light Induced Kinetic Effects on Atoms, Ions, and Molecules*, edited by L. Moi, S. Gozzini, C. Gabbanini, E. Arimondo, and F. Strumia (ETS Editrice, Pisa, 1991), pp. 5–24.
  - [11] C. Cohen-Tannoudji, in *Les Houches, Session LIII, Systèmes Fondamentaux en Optique Quantique/Fundamental Systems in Quantum Optics*, edited by J. Dalibard, J. M. Raimond, and J. Zinn-Justin (Elsevier, Amsterdam, 1992), pp. 1–164.
  - [12] J. Jersblad, H. Ellmann, K. Støchkel, A. Kastberg, L. Sanchez-Palencia, and R. Kaiser, *Phys. Rev. A* **69**, 013410 (2004).
  - [13] Y. Sortais, S. Bize, C. Nicolas, A. Clairon, C. Salomon, and C. Williams, *Phys. Rev. Lett.* **85**, 3117 (2000).
  - [14] T. W. Hodapp, C. Gerz, C. Furtlehner, C. I. Westbrook, W. D. Phillips, and J. Dalibard, *App. Phys. B: Lasers Opt.* **60**, 135 (1995).
  - [15] E. Lutz, *Phys. Rev. A* **67**, 051402(R) (2003).
  - [16] F. Bardou, J.-P. Bouchaud, A. Aspect, and C. Cohen-Tannoudji, *Lévy Statistics and Laser Cooling* (Cambridge University Press, Cambridge, 2002).
  - [17] J. Javanainen, *Phys. Rev. A* **46**, 5819 (1992).
  - [18] K. Mølmer and C. I. Westbrook, *Laser Phys.* **4**, 872 (1993).
  - [19] Y. Castin and J. Dalibard, *Europhys. Lett.* **14**, 761 (1991).
  - [20] L. Sanchez-Palencia, P. Horak, and G. Grynberg, *Eur. Phys. J. D* **18**, 353 (2002).
  - [21] G. Raithel, G. Birkl, A. Kastberg, W. D. Phillips, and S. L. Rolston, *Phys. Rev. Lett.* **78**, 630 (1997).
  - [22] G. Raithel, G. Birkl, W. D. Phillips, and S. L. Rolston, *Phys. Rev. Lett.* **78**, 2928 (1997).
  - [23] F.-R. Carminati, M. Schiavoni, L. Sanchez-Palencia, F. Renzoni, and G. Grynberg, *Eur. Phys. J. D* **17**, 249 (2001).
  - [24] F.-R. Carminati, L. Sanchez-Palencia, M. Schiavoni, F. Renzoni, and G. Grynberg, *Phys. Rev. Lett.* **90**, 043901 (2003).
  - [25] L. Sanchez-Palencia, M. Schiavoni, F.-R. Carminati, F. Renzoni, and G. Grynberg, *J. Opt. Soc. Am. B* **20**, 925 (2003).
  - [26] J. Jersblad, H. Ellmann, and A. Kastberg, *Phys. Rev. A* **62**, 051401(R) (2000).
  - [27] H. Ellmann, J. Jersblad, and A. Kastberg, *Eur. Phys. J. D* **13**, 379 (2001).
  - [28] Y. Castin and K. Mølmer, *Phys. Rev. Lett.* **74**, 3772 (1995).
  - [29] D. A. Steck, *Cesium D line data*, Technical Report No. LA-UR-03-7943, Los Alamos National Laboratory (2003), <http://steck.us/alkalidata/>.
  - [30] J. Dalibard and C. Cohen-Tannoudji, *J. Opt. Soc. Am. B* **6**, 2023 (1989).

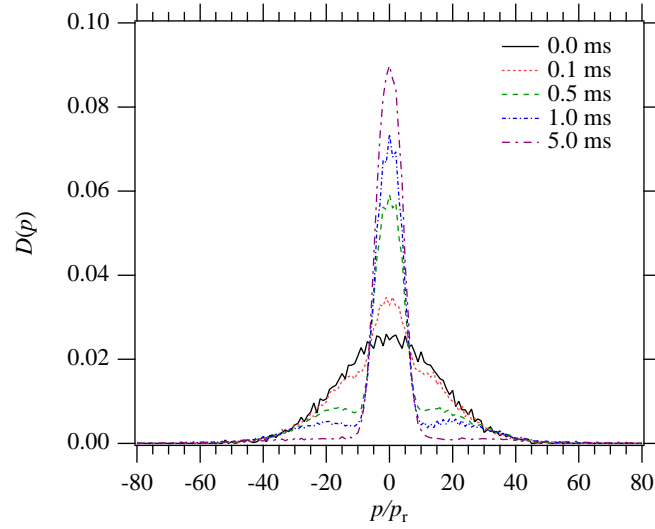


FIG. 1: Simulated momentum distribution [see eq. (1)] at different lattice times, for  $\Delta = -10\Gamma$  and  $U_0 = 127E_r$ .

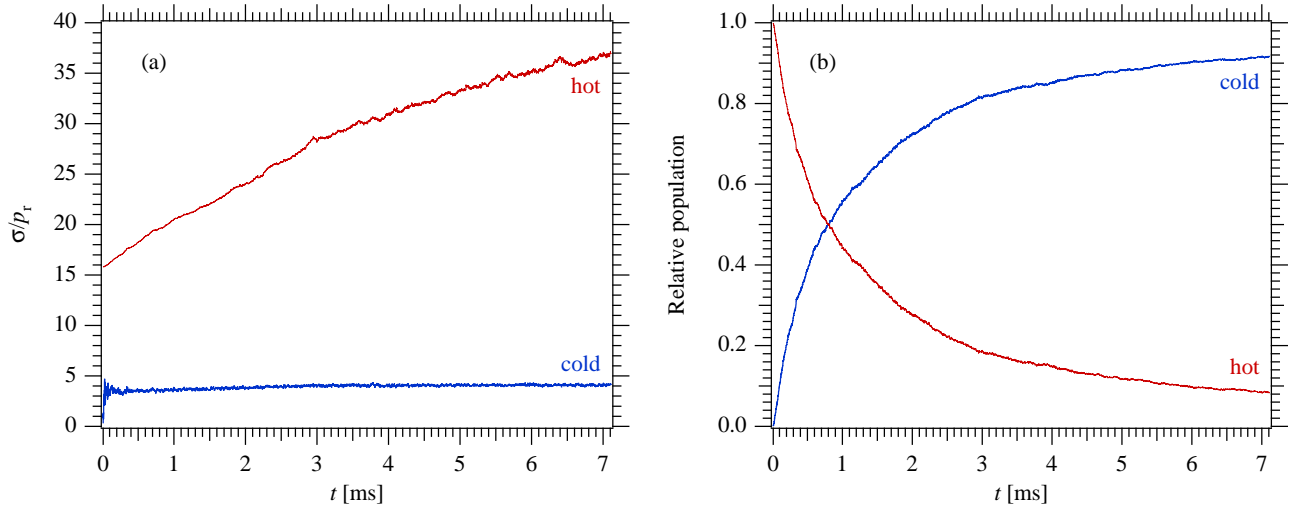


FIG. 2: Time dependence of the Gaussian fit parameters [see eq. (2)] for the cold and hot modes, for the simulated data shown in fig. 1: (a) widths  $\sigma_{\text{cold}}$  and  $\sigma_{\text{hot}}$ ; (b) relative populations.

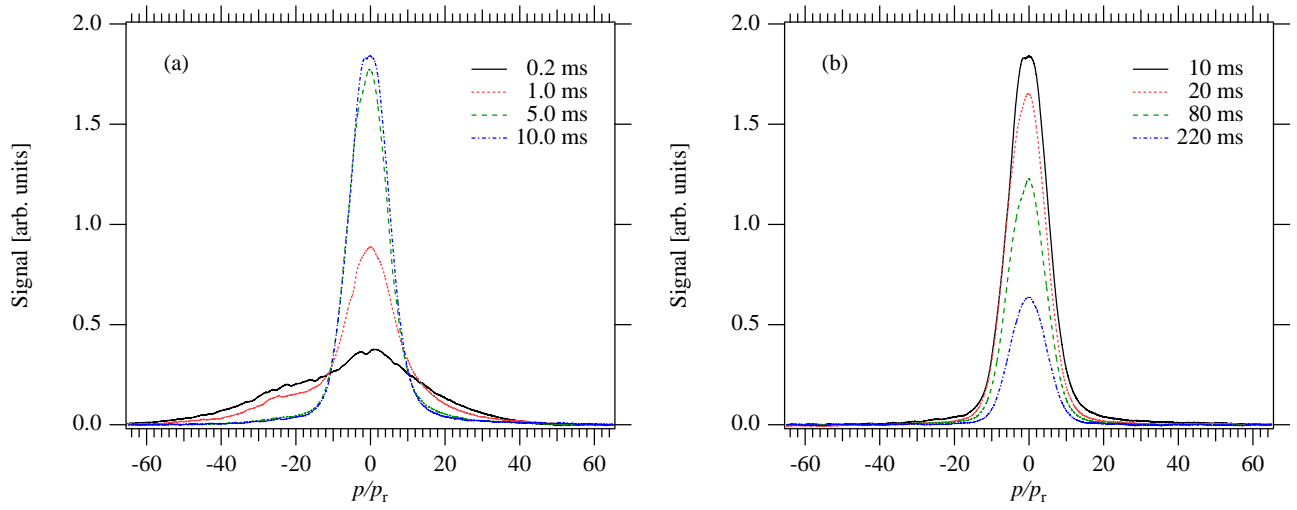


FIG. 3: Experimental momentum distribution at different lattice times, for  $\Delta = -12.6\Gamma$  and  $U_0 = 217E_r$ .

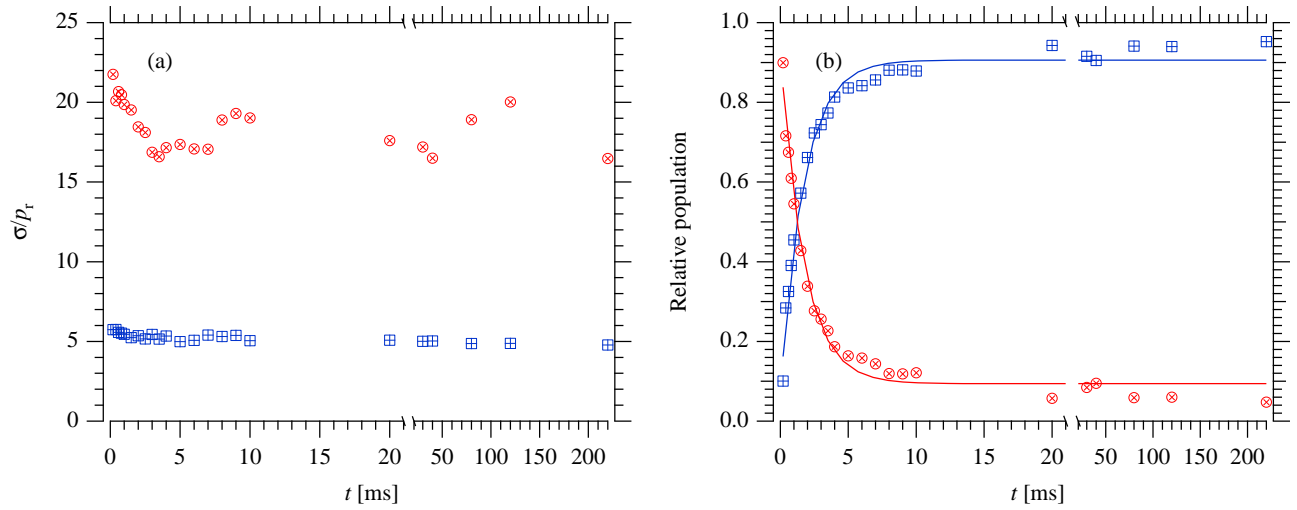


FIG. 4: Time dependence of the Gaussian fit parameters [see eq. (2)] for the cold (squares) and hot (circles) modes, for the experimental data shown in fig. 3. (a) Widths  $\sigma_{\text{cold}}$  and  $\sigma_{\text{hot}}$ . (b) Relative populations, with fits to exponential functions (solid lines). Note that there is a scale change in the time axis.

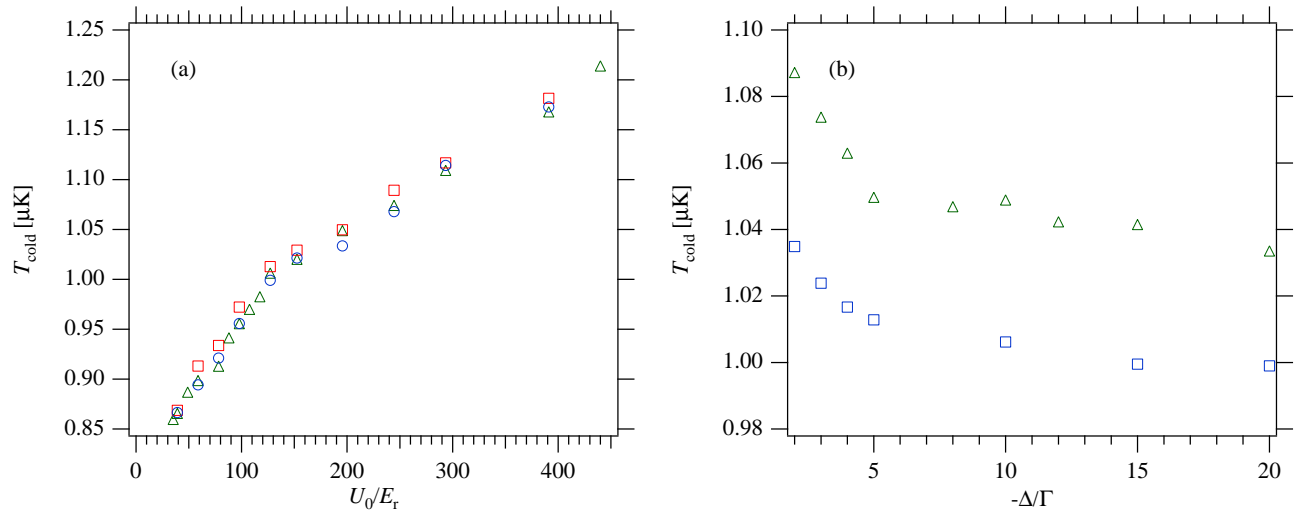


FIG. 5: Temperature of the cold mode: (a) as a function of the potential depth, for detunings of  $-5\Gamma$  (squares),  $-10\Gamma$  (triangles), and  $-20\Gamma$  (circles); (b) as a function of detuning, for well depths of  $127E_r$  (squares) and  $196E_r$  (triangles).